Cationic Order–Disorder in Double Scheelite Type Oxides: the Case Study of Fergusonite La 2 SiMoO 8

Philippe Lacorre, Antoine Pautonnier, Sandrine Coste, Maud Barré, Emilie Béchade, Emmanuelle Suard

Cationic Order–Disorder in Double Scheelite Type Oxides: the Case Study of Fergusonite La_2SiMoO_8

Philippe Lacorre,* Antoine Pautonnier, Sandrine Coste, Maud Barré, Emilie Béchade, and Emmanuelle Suard

ABSTRACT: Up to now, the possible occurrence of a cationic ordering on the tetrahedral sublattices of stoichiometric double scheelite-type oxides was not settled, with somewhat contradictory X-ray diffraction and optical measurements [Blasse, G. *J. Inorg. Nucl. Chem.* **1968**, *30*, 2091]. Using two different synthesis routes, both ordered and disordered forms of fergusonite La_2SiMoO_8 were prepared. The crystal structure of the ordered form was determined using powder X-ray and neutron diffraction, which clearly evidence a tridimensional ordering between $[SiO_4]$ and $[MoO_4]$ tetrahedra. The crystal chemistry of ordered double sheelite-type $La^{III}_2(Si^{IV}O_4)(Mo^{VI}O_4)$ can be seen as an intermediate between those of simple regular scheelite or fergusonite $Ln^{III}(Nb^{V}O_4)$ and of ordered triple scheelite $Bi^{III}_3(Fe^{III}O_4)(Mo^{VI}O_4)_2$. The structure of the disordered La_2SiMoO_8 phase was analyzed using powder X-ray diffraction. A few small and larger diffraction peaks or bumps are observed in addition to the sharper peaks of a simple fergusonite cell. DIFFaX and FAULTS programs helped showing that these faint peaks originate from stacking faults between 2D ordered layers. The intermediate 2D–3D nature of SiO_4/MoO_4 ordering in seemingly disordered compounds might explain the previous discrepancy between optical and X-ray diffraction measurements.

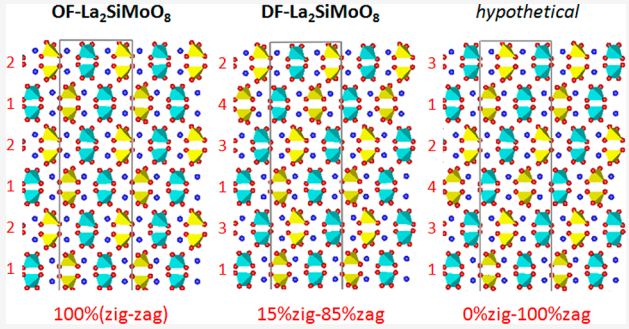

1. INTRODUCTION

Materials with a scheelite-type structure are extensively studied due to the numerous properties they can exhibit in domains such as luminescence, ferroelectricity, magnetism, ionic conduction, and catalysis, among others. More particularly, molybdate and tungstate based scheelites have excellent optical properties and are currently used as laser materials, scintillation detectors, and phosphors (see introductions of refs 1 and 2).

These properties are partly due to the ability of the ABO_4 scheelite structure to accommodate ions with various sizes and charges. In original scheelite $CaWO_4$, the Ca^{2+} cation (A site) is in 8-fold coordination (square antiprism), whereas W^{6+} (B site) is in tetrahedral coordination. This structural type is built up from isolated files of isolated $[BO_4]$ tetrahedra forming corrugated layers interleaved with corrugated A planes (a projection of which is presented later on in Figure 5a for A = Ce^{3+} and B = Nb^{5+}). Various partial or total substitutions are possible on both sites involving mono- (alkali element, Ag, Tl, NH_4), di- (alkaline earth, Cd, Pb, Eu), tri- (rare earth, Bi), or tetravalent (Zr, Hf, Th, Ce, U) elements on the A site or di- (Zn), tri- (Fe, Ga), tetra- (Ti, Si, Ge), penta- (As, V, Nb, Ta, Mo), hexa- (Cr, Mo, S), hepta- (Re, Tc, Ru, I), or octavalent (Os) elements on the B site.[3] Substitutions are also possible on the anionic site by mono- (F) or trivalent (N) anions. Note that both disorder and tetrahedral distortions are thought to play a role in the photoluminescence emission of such powder materials.[1]

The scheelite structural arrangement can also accommodate several types of nonstoichiometries on cationic and anionic sites[4,5] and adopt different symmetries, including incommensurability (modulated structures).[6] In stoichiometric compounds, most common symmetries are tetragonal, like in original scheelite $CaWO_4$ (space group $I4_1/a$), or monoclinic, like in fergusonite $YNbO_4$ (space group $C2/c$ or nonstandard $I2/a$), a distorted kind of scheelite.[7]

The occurrence of two cations with different charges and sizes on the same site of scheelite brings about the question of possible superstructure due to cationic ordering. On the A site, such an ordering has been clearly evidenced when the difference in size and charge is large enough; otherwise there is cationic disorder on the same crystallographic site (simple

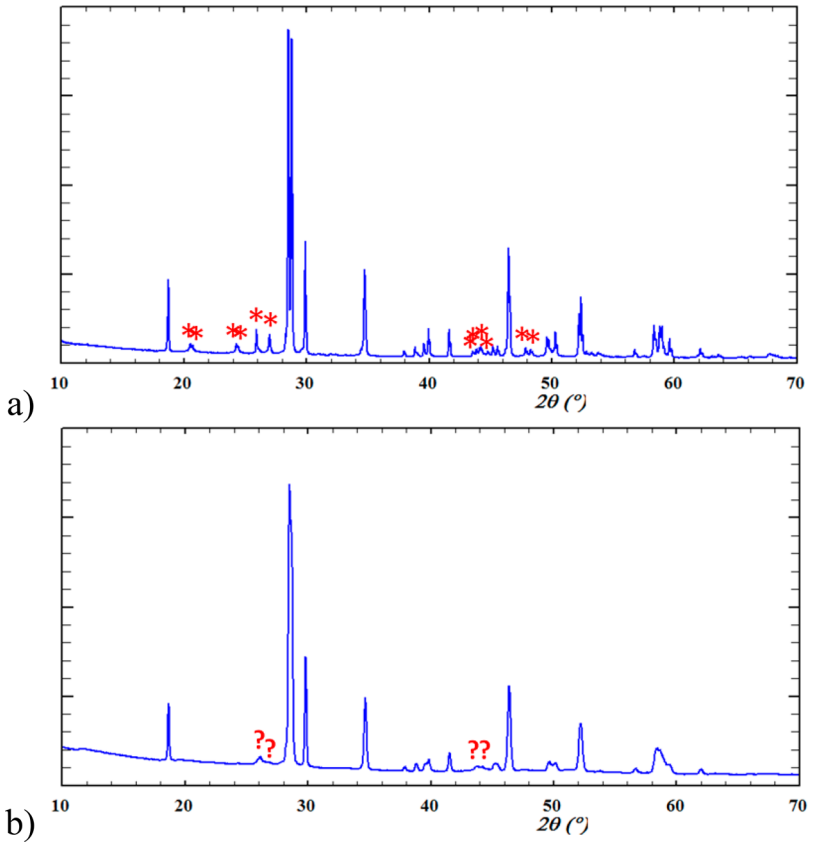

Figure 1. X-ray diffraction patterns of OF-La_2SiMoO_8 prepared by solid state reaction (a) and of DF-La_2SiMoO_8 prepared by polyol process (b). Red stars and question marks indicate additional peaks or bumps relative to a simple monoclinic fergusonite cell (see text).

cell). In $A^+A'^{3+}[Mo(W)O_4]_2$, a difference in size $r(A^+)/r(A'^{3+})$ larger than 1.32 is necessary to generate ordering/superstructure.[8,9] This is the case for instance in molybdates with AA′ being KSm, KEu, RbLa, or RbBi. The situation is not as clear for the ordering of B cations in tetrahedral coordination. The only reported clear cases of B cation ordering concern trivalent iron or gallium and hexavalent molybdenum, in compounds $Bi_3[Fe(Ga)O_4][MoO_4]_2$: they crystallize as ordered triple scheelites upon annealing of a low temperature disordered form.[10] With tetravalent cations T = Si, Ge, or Ti, series of double scheelite exist with formula A_2TMoO_8 or A_2TWO_8, A being a rare earth.[11] Most appear to be disordered scheelites (or fergusonites), except maybe with silicon, but here X-ray and optical measurements lead to somewhat contradictory inferences, X-ray diffraction suggesting disorder whereas emission lines indicate long-range order. Therefore, no firm conclusion was reached.

The current study addresses the above issue. We were able, using solid state and liquid phase routes, to prepare ordered and disordered samples of La_2SiMoO_8. In this paper, we used neutron and X-ray powder diffraction to determine the crystal structure of the ordered phase and analyze the disordered arrangement, as an attempt to understand the discrepancy of previous studies.

2. EXPERIMENTAL SECTION

2.1. Synthesis. Two different synthesis routes were used to get powder samples of the ordered and disordered forms of fergusonite La_2SiMoO_8. The ordered phase was obtained by heating up a stoichiometric mixture of the commercial elementary oxides La_2O_3, SiO_2, and MoO_3 first at 500 °C overnight (to avoid MoO_3 sublimation through a low temperature reaction with La_2O_3), then up to 1200 °C, the final synthesis temperature, with intermediate grindings. Before weighing starting oxides, La_2O_3 was annealed for a night at 1000 °C in order to remove traces of carbonate and hydrate.

The disordered phase was prepared by soft chemistry polyol synthesis according to the following procedure. The reagents, lanthanum acetate sesquihydrate ($La(OOCCH_3)_3{\cdot}1.5H_2O$, Alfa Aesar 99.99%), ammonium molybdate ($(NH_4)_2Mo_2O_7$, Alfa Aesar 56.5% in Mo), and tetraethyl orthosilicate ($Si(OCH_2CH_3)_4$, Alfa Aesar 98%) were added in stoichiometric proportions with a concentration of 0.2 mol·L^{-1} of metallic cations in 30 mL of diethylene glycol ($(HOCH_2CH_2)_2O$, Alfa Aesar 99%). Then, 2 mL of ammonia (NH_3 25%, Scharlau) was added to basify the solution, then refluxed for 3 h in a flask thermostated at 245 °C in a sand bath. After cooling at room temperature, the solution was centrifuged to collect the precipitate formed. The maximum of solvent traces was removed by multiple washings and centrifugations in ethanol before drying the washed precipitate in an oven at 110 °C for a night. The amorphous precursor thus obtained was then ground and heated in a furnace at 1000 °C for 12 h, to obtain a powder of the crystallized disordered form of fergusonite La_2SiMoO_8. The ordered form can also be obtained by annealing the disordered form at 1200 °C.

Note that La_2SiMoO_8 can also be obtained by annealing of an intimate stoichiometric mixture of $La_2Si_2O_7$[12] and $La_2Mo_2O_9$.[13] In this case, the $La_2Si_2O_7$ phase was previously prepared by solid-state reaction between high-purity La_2O_3 (99.9% Sigma-Aldrich) and amorphous silica SiO_2 (Cerac, > 99.9%). The La_2O_3 reagent was dried, as for the ordered phase La_2SiMoO_8, to determine the appropriate amount of reagent. Both oxides were mixed in a 1:2 (La_2O_3/SiO_2) molar ratio by attrition (Union Process-Szegvari attritor system) in water for 2.5 h at 450 rpm in a Teflon bowl, with zirconia balls of 1 mm and 2 mm in diameter. Dried powder was calcined in Pt crucibles at 1200 and 1500 °C for 10 h in air at a heating rate of 10 °C.min^{-1}.

2.2. Powder Diffraction and Structure Determination. The powder diffraction patterns were recorded at room temperature on Bragg–Brentano diffractometers, PANalytical X'Pert and/or Empyrean (X-ray, ordered and disordered phases), and the ILL high resolution powder diffractometer D2B (neutron, ordered phase). The details of data collection are reported in Table 1.

Crystal cell determination and refinement were performed using programs DICVOL[14] and CELREF,[15] respectively, using X-ray diffraction patterns. Heavy cation positioning in the ordered phase was determined using the structure solution program SHELXS (direct methods)[16] on X-ray diffraction intensities extracted from the powder pattern by the program FULLPROF (whole pattern decomposition by Le Bail fitting procedure).[17,18] Further atomic positioning and structure refinement were performed through alternate use of SHELXL (Fourier syntheses)[16] and FULLPROF (Rietveld refinement)[19] programs. Structural analysis of the disordered form was carried out with the help of programs DIFFaX,[20] DIFFaX2FAULTS, and FAULTS,[21] which were used to simulate X-ray powder diffraction patterns of crystallites built up from stacking faults of selected atomic layers of the ordered form. A discussion on the integration of the different structural software is provided while analyzing the results. All throughout this work, the line profile used to model peak shapes during refinements is Thompson–Cox–Hastings pseudo-Voigt. Structural drawings were made using structure visualization program DIAMOND[22] and FullProf Studio.[23]

3. RESULTS

3.1. Ordered and Disordered Forms of Fergusonite La_2SiMoO_8. Following the assertion by Blasse[11] about the existence of a fergusonite (monoclinic distortion of scheelite) with the composition La_2SiMoO_8, we were able to synthesize two different pure polymorphs with such a composition and structural type: the first one was prepared by the solid state reaction at 1200 °C of a mixture of elementary oxides and the second one by soft chemistry with final annealing at a lower temperature, around 1000 °C (see Experimental Section for synthesis details).

X-ray diffraction patterns of both phases are shown in Figure 1. In the sample prepared by the solid state reaction, the X-ray diffraction pattern of which is shown in Figure 1a, extra diffraction peaks relative to the simple fergusonite cell given by Blasse are clearly visible (stars in Figure 1a). They can be indexed after doubling the *a* parameter of simple fergusonite cell, which strongly suggests a cationic ordering between molybdenum and silicon.

The X-ray diffraction pattern of the other sample, prepared by a polyol process, is shown in Figure 1b. Extra diffraction peaks, bumps, or streaks are also visible (question marks in Figure 1b), but much fewer and weaker than in the ordered phase. We therefore consider this phase a disordered fergusonite version of the La_2SiMoO_8 polymorph.

In the following, the ordered and disordered fergusonite phases will be called OF-La_2SiMoO_8 and DF-La_2SiMoO_8, respectively. The structure of both phases will now be determined and analyzed using X-ray and neutron powder diffraction.

3.2. Ordered OF-La_2SiMoO_8: Structure and Discussion. *3.2.1. OF-La_2SiMoO_8 Structural Determination.* The crystal structure OF-La_2SiMoO_8 was determined using first powder X-ray diffraction for cation positioning then powder neutron diffraction for oxide ion localization. The structural determination procedure is described in the Experimental Section. Extinction conditions suggesting the presence of a 2_1 screw axis, first attempts of atomic localization and refinement were carried out in space group $P2_1$. A close analysis of cationic positions in this space group showed the existence of a *c* glide plane perpendicular to the screw axis. Subsequent structural refinements were therefore carried out in space group $P2_1/c$. Powder neutron diffraction was used to localize oxide ions. There are two independent La atoms, one Si, one Mo, and eight O, all of them being located on general positions 4e of space group $P2_1/c$.

The reliability factors of the refined structure and the cell parameters and atomic positions of OF-La_2SiMoO_8 are given in Tables 1 and 2, respectively, and a result of the fit in Figure 2. Figure 3 shows the crystal structure of the ordered fergusonite from different viewpoints. Isolated $[SiO_4]$ and $[MoO_4]$ tetrahedra form, stacked along the *a* cell axis, alternating corrugated layers interleaved with corrugated lanthanum planes. This ordering is responsible for the doubling of the a cell parameter relative to a simple fergusonite cell. To our knowledge, this is the first clear evidence of the existence of a 3D ordering in a double scheelite $A_2BB'O_8$.

Table 1. Conditions of D2B Neutron Data Collection for the Structural Refinement of Ordered La_2SiMoO_8

wavelength	1.5952 Å
θ range	7–155.5°
step-scan increment	0.05°
monitor/counts	550000.00

Table 2. Crystallographic Parameters of OF-La_2SiMoO_8, from Neutron Diffraction Refinement[a]

atom	site	*x*	*y*	*z*	occ	*B* (Å^2)
La1	4e	0.661(1)	0.873(1)	0.489(3)	1	0.8(3)
La2	4e	0.100(1)	0.629(1)	0.999(3)	1	1.0(3)
Mo	4e	0.623(3)	0.128(1)	0.007(5)	1	0.7(2)
Si	4e	0.126(4)	0.378(2)	0.513(7)	1	−0.2(3)
O1	4e	0.501(2)	0.288(2)	0.355(4)	1	0.4(4)
O2	4e	0.001(2)	0.193(2)	0.906(6)	1	1.7(5)
O3	4e	0.182(2)	0.030(2)	0.787(5)	1	1.8(5)
O4	4e	0.254(2)	0.191(2)	0.085(5)	1	0.7(4)
O5	4e	0.554(2)	0.049(2)	0.247(4)	1	0.9(4)
O6	4e	0.745(2)	0.204(2)	0.144(4)	1	0.5(4)
O7	4e	0.082(2)	0.056(2)	0.282(4)	1	0.8(4)
O8	4e	0.307(2)	0.949(2)	0.255(5)	1	1.3(5)

[a]Space group: $P2_1/c$ (no. 14), Z = 4. a = 10.3236(5) Å, b = 11.9647(5) Å, c = 5.1653(3) Å, β = 90.737(3)° (volume = 637.96(5) Å^3). Fit using 1229 reflections with pseudo-Voigt peak shape and 68 refined parameters: R_{Bragg} = 7.45%, R_p = 11.4%, R_{wp} = 12.3%, R_{exp} = 3.09%.

3.2.2. Comparison with Other Ordered Scheelite-Type Structures. As presented in the Introduction, other ordered scheelite-type structures have been evidenced either as double scheelites involving A cations like in $A^+A'^{3+}[Mo(W)O_4]_2$ or as triple scheelites involving B cations like in $Bi_3[Fe(Ga)O_4]$-$[MoO_4]_2$. In this section, we compare the OF-La_2SiMoO_8 structure with these two different types of orderings.

3.2.2.1. $AA'B_2O_8$. Klevtsov et al.[8] and Kolesov et al.[9] have shown that in scheelites $AA'B_2O_8$, when a difference in charge of 2 exists between A and A′ (typically A^+ and A'^{3+}) and the difference in size $r(A^+)/r(A'^{3+})$ is larger than 1.32, an ordering occurs between A and A′ cations. This is typically the case in $A^+A'^{3+}[Mo(W)O_4]_2$ with AA′ being KSm, KEu, RbLa, or RbBi.

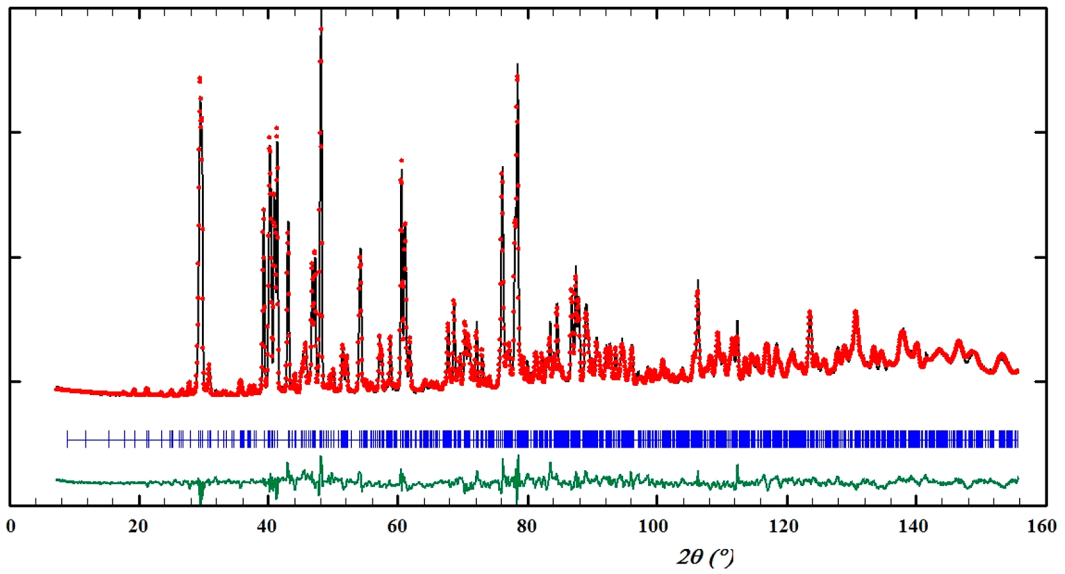

Figure 2. Result of the structural fit of the neutron diffraction pattern of OF-La_2SiMoO_8 using parameters given in Tables 1 and 2. Observed, calculated, and difference plots in black, red, and green, respectively. Blue vertical bars indicate reflection positions.

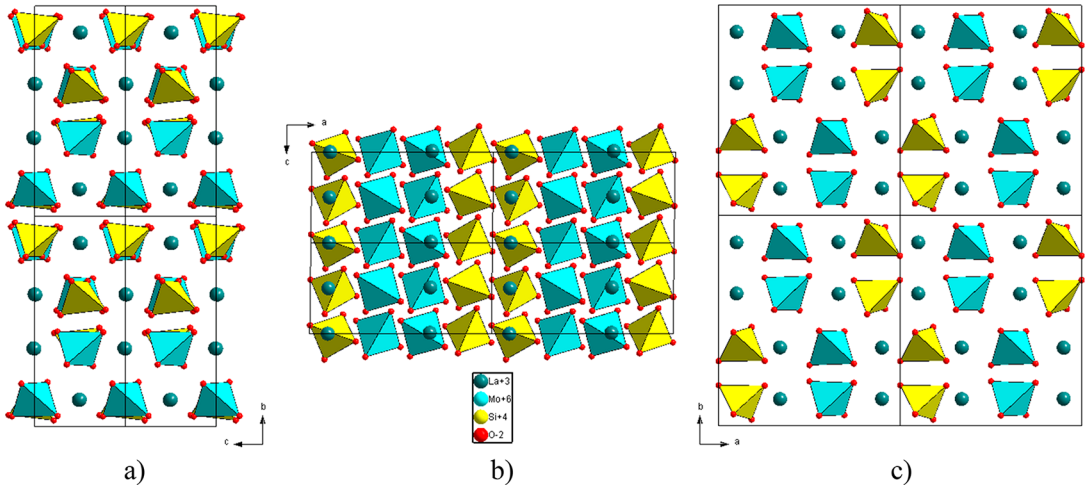

Figure 3. Crystal structure of OF-La_2SiMoO_8 projected along *a*, *b*, and *c* cell parameters. [SiO_4] and [MoO_4] coordination tetrahedra are in yellow and cyan, respectively.

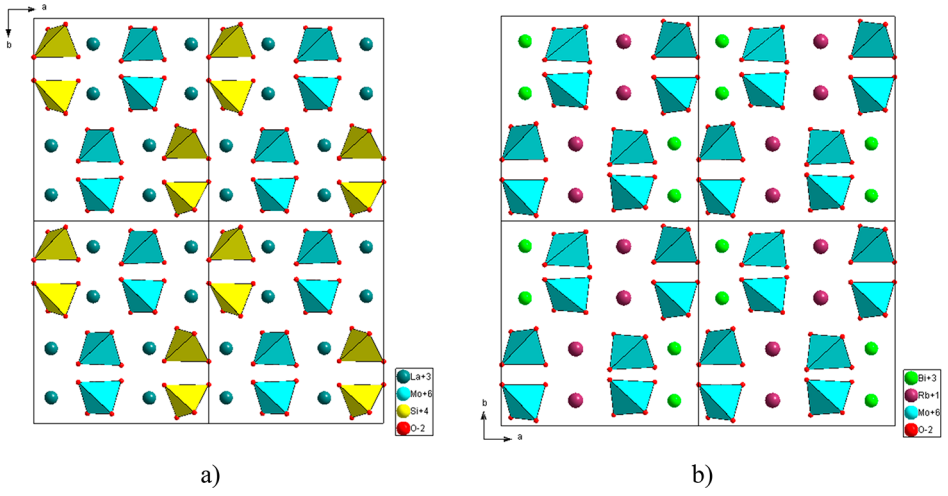

Figure 4. Comparison between the structures of (a) OF-La_2SiMoO_8 with ordering between Si^{4+} (yellow) and Mo^{6+} (cyan) and (b) $RbBiMo_2O_8$ with ordering between Rb^{+} (violet) and Bi^{3+} (green).

Table 3. Comparison between Cationic Coordinates in La_2SiMoO_8 (LSM) and in $RbBiMo_2O_8$ (RBM, in Italic),[24] between Cations of the Same Type AA or BB (Left) and between Cations of Different Types AB or BA (Right)

	x (LSM) *x (RBM)*	y (LSM) *y (RBM)*	z (LSM) *z (RBM)*		$1/4 + x$ (LSM) *x (RBM)*	y (LSM) *y (RBM)*	$1/2 + z$ (LSM) *z (RBM)*
La1	0.66	0.87	0.49	La1	0.91	0.87	0.99
Rb	*0.62*	*0.88*	*0.48*	*Mo1*	*0.89*	*0.89*	*0.98*
La2	0.10	0.63	0.00	La2	0.35	0.63	0.50
Bi	*0.12*	*0.62*	*0.01*	*Mo2*	*0.34*	*0.65*	*0.50*
Si	0.13	0.38	0.51	Si	0.38	0.38	0.01
Mo1	*0.11*	*0.39*	*0.52*	*Rb*	*0.38*	*0.38*	*0.02*
Mo	0.62	0.13	0.01	Mo	0.87	0.13	0.51
Mo2	*0.66*	*0.15*	*0.0*	*Bi*	*0.88*	*0.12*	*0.49*

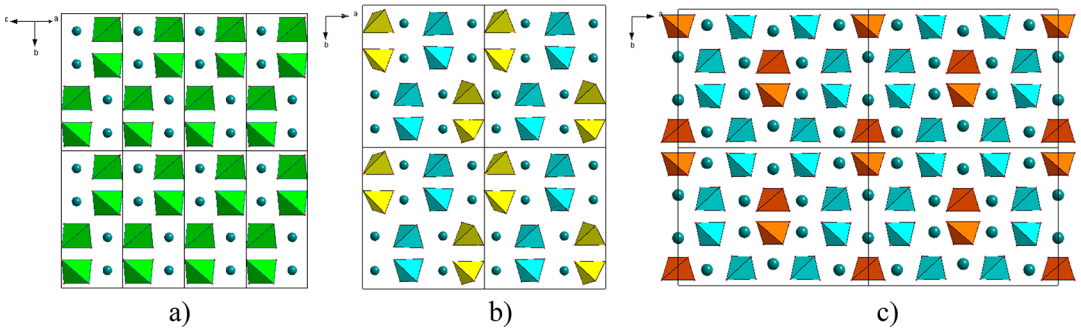

Figure 5. Comparison between the structures of $CeNbO_4$ (a, simple scheelite type), OF-La_2SiMoO_8 (b, double scheelite type), and $Bi_3FeMo_2O_{12}$ (c, triple scheelite type). Tetrahedra colors: $[Fe^{3+}O_4]$ in orange, $[Si^{4+}O_4]$ in yellow, $[Nb^{5+}O_4]$ in green, and $[Mo^{6+}O_4]$ in cyan.

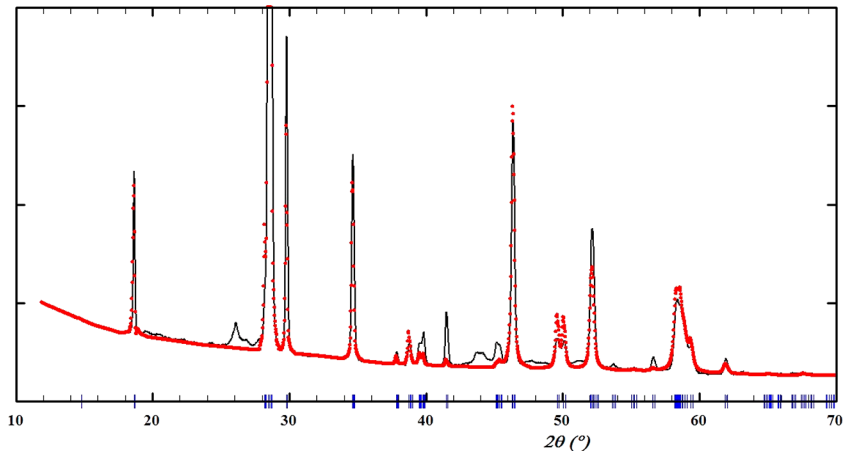

Figure 6. Fit of the X-ray diffraction pattern of DF-La_2SiMoO_8 with a simple fergusonite model and Si and Mo statistically distributed in the same tetrahedral site (black line = observed; red dots = calculated).

Figure 4 compares the structure of OF-La_2SiMoO_8 to the one of $RbBiMo_2O_8$.[24] It can be clearly seen that the ordering of cations with a difference in charge of 2 is of the same type in both structures.

In order to show that the similitude between the two arrangements not only develops along one direction but is three-dimensional in nature, we compare in Table 3 the cationic positions in both structures (after appropriate overall shifts to bring cells in correspondence).

3.2.2.2. $A_3BB'_2O_{12}$. Concerning ordering between B cations in scheelite type structures, as mentioned in the Introduction, the only other clear examples of 3D ordering were observed with trivalent Fe^{3+} and Ga^{3+} cations in the high temperature forms of $Bi_3[Fe(Ga)O_4][MoO_4]_2$, resulting from the annealing of low temperature disordered forms.[10] Figure 5 shows how OF-La_2SiMoO_8 naturally inserts in between $CeNbO_4$ and $Bi_3FeMo_2O_{12}$ in a general tetrahedral ordering scheme of scheelite type.

3.3. Disordered DF-La_2SiMoO_8: Structure and Discussion. *3.3.1. Completely Disordered Model in a Simple Fergusonite Cell.* The most simple disordered model of DF-La_2SiMoO_8 is to consider it as a simple monoclinic fergusonite as did Blasse in his initial paper.[11] Using the more convenient *I*2/*a* space group, which allows direct comparison with the double cell of DF-La_2SiMoO_8, we fitted the X-ray diffraction pattern of the disordered phase with a statistical model of Mo and Si distribution on the same tetrahedral site. The cell parameters are close to those of OF-La_2SiMoO_8 in a simple cell, with a slightly different monoclinic distortion, *a* and *c* being more split apart but the monoclinic angle closest to 90°

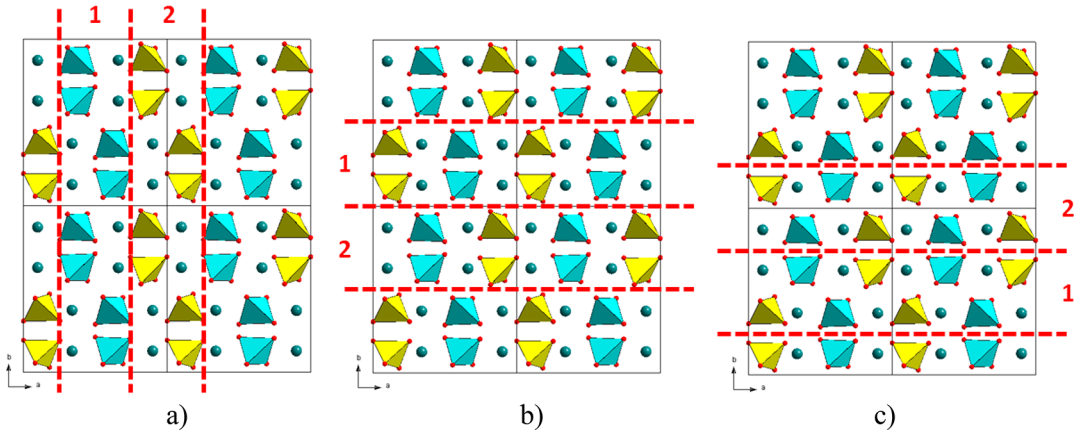

Figure 7. Different types of layers considered for the three stacking fault models of DF-La_2SiMoO_8: along the *a* axis (a) and along the *b* axis (b and c). Note that the same numbering represents different types of layers depending on the model. See the text for details.

and volume ∼ 0.3% larger, namely, a = 5.177(2) Å, b = 11.984(3) Å, c = 5.168(2) Å, β = 90.50(1)°, volume = 320.6(2) Å^3.

As anticipated, the fit is not very good, especially for the extra small peaks which do not fit in a simple monoclinic cell (see Figure 6). The presence of extra small peaks and bumps clearly different from (although maybe not totally disconnected to) those of OF-La_2SiMoO_8 (see Figure 1) incited us to consider other types of disordering models.

3.3.2. Stacking Faults Models. In section 3.2.1., the structure of OF-La_2SiMoO_8 has been described as alternating corrugated layers of isolated [SiO_4] and [MoO_4] tetrahedra interleaved with corrugated lanthanum planes, stacked along the *a* axis (see Figure 3c). Such a stacking mode of layers filled either with [SiO_4] or with [MoO_4] tetrahedra might be at the origin of stacking faults consistent with the absence of any long-range tetrahedral ordering along one direction, and its presence along the others. It could explain the existence of fainter extra diffraction peaks relative to a fully disordered sample. In order to test this hypothesis, we used the computer program DIFFaX to generate different types of stacking faults in OF-La_2SiMoO_8 layers and analyze their incidence on the powder X-ray diffraction pattern. Since the order/disorder process concerns mainly Si^{4+} and Mo^{6+} cations, X-ray diffraction appears the most appropriate tool to study it due to the large contrast between these elements.

Different types of layers were considered, within three modes of stacking along either the a or the *b* axis: along the *a* axis, two layers containing only either [SiO_4] or [MoO_4] tetrahedra (layers 1 and 2 in Figure 7a), stacked randomly; along the *b* axis, four layers containing facing rows of isolated [SiO_4] or [MoO_4] tetrahedra (layers 1 and 2 in Figure 7b, together with 4 and 3, their respective shifts by $a/2$), stacked randomly; and along the *b* axis, four layers containing serrated rows of isolated [SiO_4] or [MoO_4] tetrahedra (layers 1 and 2 in Figure 7c, together with 4 and 3, their respective shifts by $a/2$), stacked randomly.

Within the DIFFaX program, layers are always stacked along the *c* axis, which implied a permutation of atomic coordinates to fit with the new reference frame. In addition to the appropriate selection of atoms in the considered layers, the monoclinic angle—although close to 90°—was taken into account (more specifically in the stacking along *a*). In any way before any random stacking computation, checks were carried out, on the proper periodic stacking of layers corresponding to the OF-La_2SiMoO_8 structure, that its powder X-ray diffraction pattern was reproduced exactly by DIFFaX. It thus validated the correctness of our layers' reconstruction.

The three different types of random stacking are shown in Figure 8. For each stacking, the two or four layers used are numbered (their configuration can be seen on the right side of the figure). We have used the DIFFaX Explicit Random stacking sequence with 1000 layers to generate samples corresponding to each stacking type, the sequences of which are given on the left part of the figure. Excerpts of 10 layers (red frames) are drawn on the right side as illustrations of the random sequences.

For each stacking, the transition probabilities between layers have been defined as follows: (a) stacking along *a* (Figure 8a), each layer 1 or 2 has a 50% probability to have either layer 1 or 2 as a neighboring layer; (b) stacking 1 along *b* (Figure 8b), each layer 1 or layer 4 has a 50% probability to have either layer 2 or 3 as neighbors, and 0% probability to have layer 1 or 4, and each layer 2 or layer 3 has a 50% probability to have either layer 1 or 4 as neighbors, and 0% probability to have layer 2 or 3; (c) stacking 2 along *b* (Figure 8c), same transition probabilities as stacking 1 with the layers of stacking 2.

In all three stackings, the corrugated lanthanum planes are kept; only rows of isolated tetrahedra [SiO_4] and [MoO_4] along the *c* axis are distributed differently, according to the layers and transition probabilities defined above.

In Figure 9, we compare the X-ray diffraction patterns generated by DIFFaX for the three stackings of Figure 8 to the X-ray diffraction pattern of DF-La_2SiMoO_8. Besides the main diffraction peaks also present in a totally disordered model, we focus on those additional faintest peaks characteristic of the irregular defective ordering. They are surrounded by ovals, either a full line when a feature is present or a dashed line when absent. It appears clearly that the stacking 1 along *b* (Figure 8b) gives the closest diffraction pattern (red in Figure 9b) to the experimental one (Figure 9a), with all features present or absent identically. Additionally, the diffraction patterns of the two other stackings have either missing and/or additional features in comparison to the experimental pattern.

The specific ordering of layers 1 and 2 in OF-La_2SiMoO_8, of the type 12121212..., results in corrugated arrangement of tetrahedral rows of [SiO_4] and [MoO_4], as depicted earlier. For convenience, let us call this type of ordered arrangement a "zigzag" arrangement of layers. In comparison, the random arrangement of Figure 8b can be considered as a statistical 50%

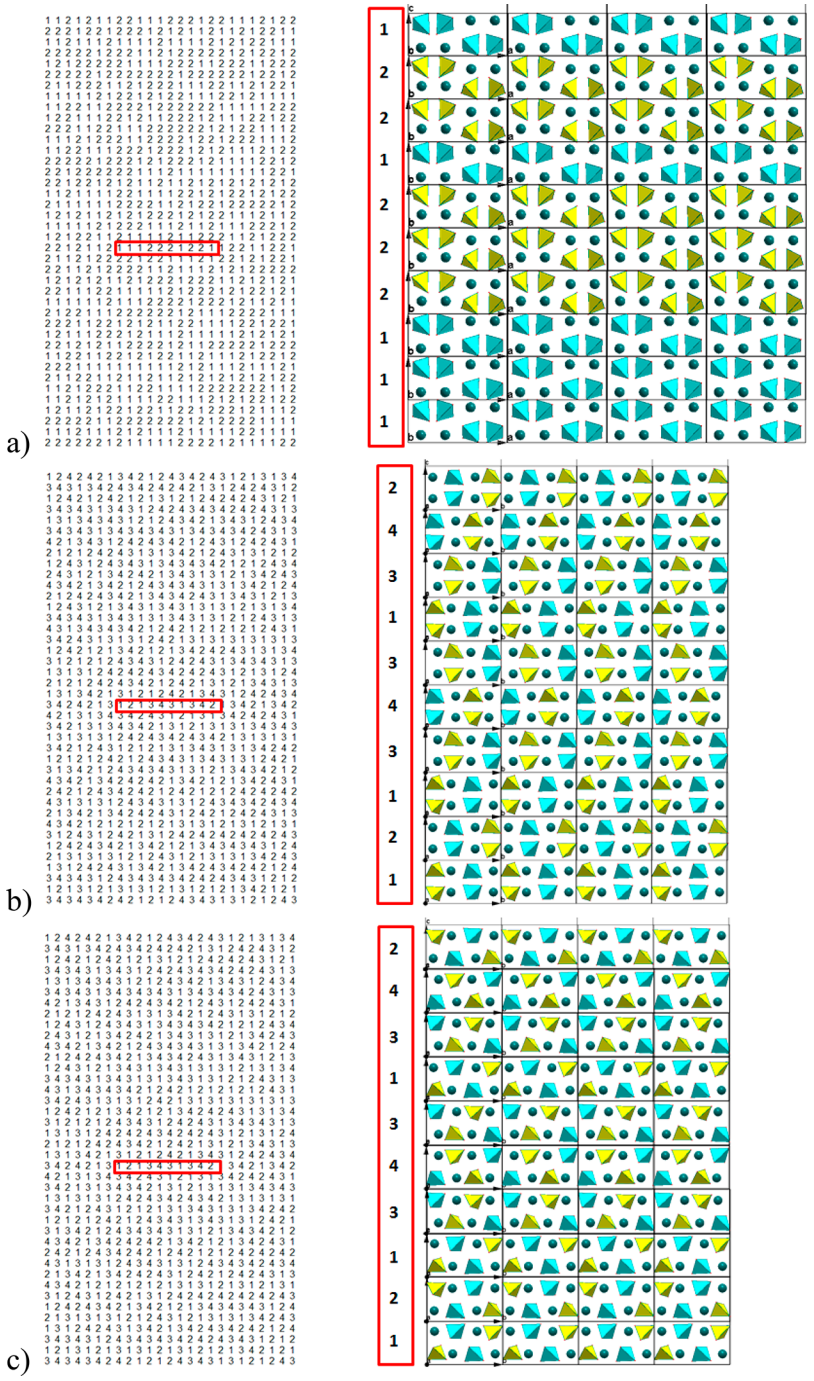

Figure 8. The three 1000 layers stackings along *a* (a) and *b* (b and c) generated by DIFFaX with transition probabilities described in the text. The left part gives the randomly computed successions of layers, while the right part shows configurations of the 10 successive layers in red frame excerpts.

zig−50% zag arrangement. When looking more carefully at the small extra diffraction peaks generated by this model, it appears that the first small generated peak around $2\theta = 26°$ is slightly shifted toward a lower angle compared to the observed diffraction pattern of DF-La_2SiMoO_8 (see Figure 10a). In order to attempt to optimize the arrangement of DF-La_2SiMoO_8, we used the program FAULTS, which allows refinement of the structural features of compounds with planar defects from their X-ray diffraction pattern.[21] Stacking input files were conveniently built from DIFFaX files by using the converter program DIFFaX2FAULTS.[21]

3.3.3. Stacking Faults Refinement. Refinements including the stacking probability of layers induced an improvement in the fit of the additional small peak, as can be seen in Figure 10b. The best agreement was obtained for a transition probability between layers of the type 15% zig−85% zag (see Figure 10b). The fit between calculated and observed patterns is not perfect (see Figure 11) and probably secondary effects would have to be taken into account, but in first approximation it is expected that the most salient features of the stacking defaults of DF-La_2SiMoO_8 have been depicted.

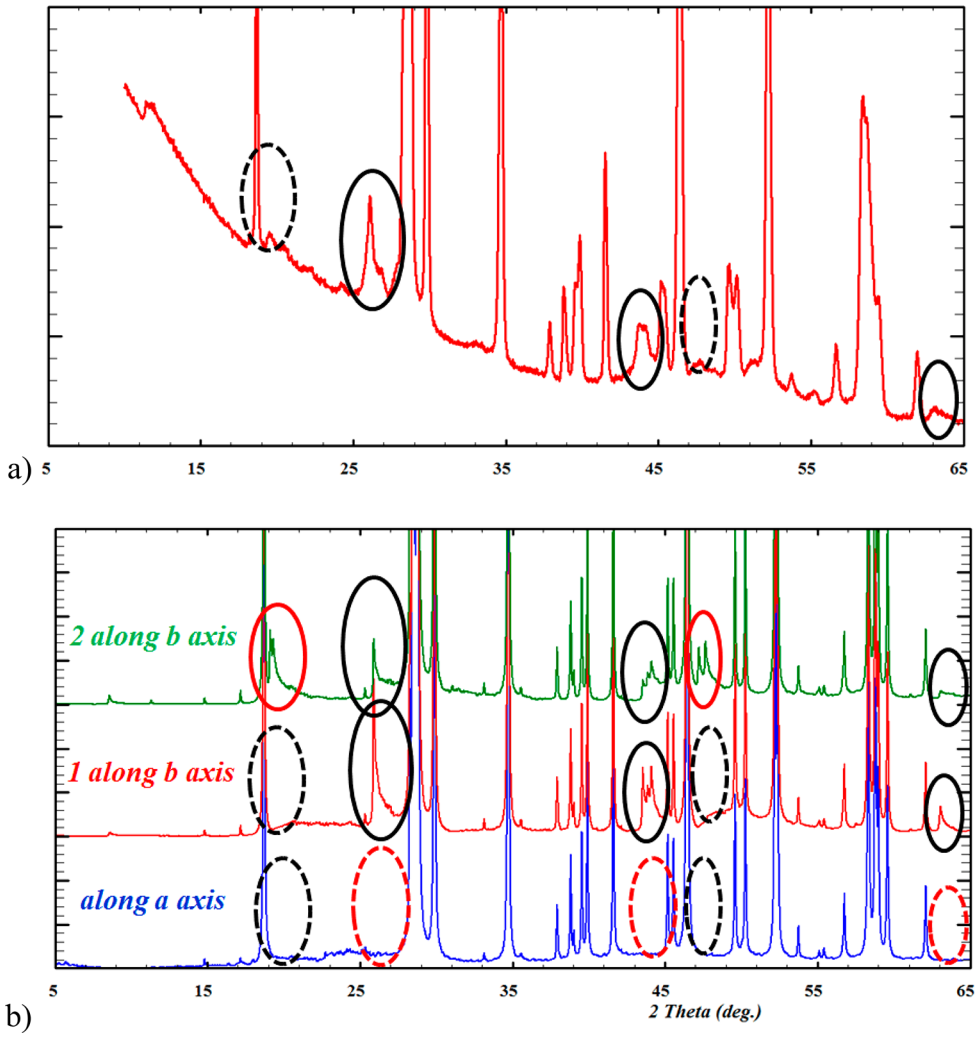

Figure 9. X-ray powder diffraction patterns of DF-La_2SiMoO_8 (a) and simulated by DIFFaX (b) for the three samples with random stacking faults of Figure 8. Main additional diffraction features relative to a fully disordered sample are surrounded by oval full lines (their absence by oval dashed lines).

Note that the 15% zig−85% zag stacking is somewhat intermediate between a 50% zig−50% zag full staking disorder and a hypothetical completely ordered 100% zag structure with diagonal arrangement of tetrahedral [SiO_4] and [MoO_4] rows (see inset of Figure 12). The X-ray diffraction pattern of this "hypothetical diagonal" structure is shown in Figure 12, where it is compared to those of DF-La_2SiMoO_8 and of the 15% zig−85% zag staking.

4. CONCLUSION

This paper was devoted to the study of the crystal structure of fergusonite, double scheelite type La_2SiMoO_8. We have shown that depending on the synthesis method and on the annealing temperature, one could get either an ordered phase OF-La_2SiMoO_8 (solid state reaction, 1200 °C), or a disordered phase DF-La_2SiMoO_8 phase (polyol synthesis, 1000 °C). The crystal structure of OF-La_2SiMoO_8 was determined using neutron powder diffraction. The silicon and molybdenum sublattices are tridimensionally ordered in corrugated planes of rows of isolated [$Si^{4+}O_4$] and [$Mo^{6+}O_4$] tetrahedra, the same way as A^+ and A^{3+} large cations in ordered double scheelites $A^+A'^{3+}[Mo(W)O_4]_2$. Also, in terms of structural series, the first tetrahedrally ordered double scheelite OF-La_2SiMoO_8≡ $La_2[SiO_4][MoO_4]$ fills perfectly the gap between simple fergusonites such as LnNbO4 and tetrahedrally ordered triple scheelites $Bi_3[Fe(Ga)O_4][MoO_4]_2$.

The structure of disordered DF-La_2SiMoO_8 was studied by X-ray powder diffraction using DIFFaX and FAULTS programs of simulation and refinement of stacking faults randomly generated in building layers of OF-La_2SiMoO_8. The best model reproduces correctly the few extra faint peaks observed in the observed diffraction pattern.

These results echo the outcome of the seminal study by Blasse, more than 50 years ago, on the crystal structure and fluorescence of compounds $Ln_2Me^{4+}Me^{6+}O_8$.[11] In the latter paper, the author questions the inability of X-ray diffraction (XRD) to detect any long-range cationic ordering, whereas fluorescence spectroscopy does. Whatever the origin of the nondetection of superstructure by XRD in Blasse's work—either the low sensitivity of the period diffractometer or disordering induced by extra chemical elements (fluorine, other rare-earth) introduced during the synthesis process—our current results provide an explanation on why a seemingly disordered material, from XRD patterns, could exhibit some kind of ordering in spectroscopic measurements. As a matter of fact, the stacking disorder we identified for DF-La_2SiMoO_8 is

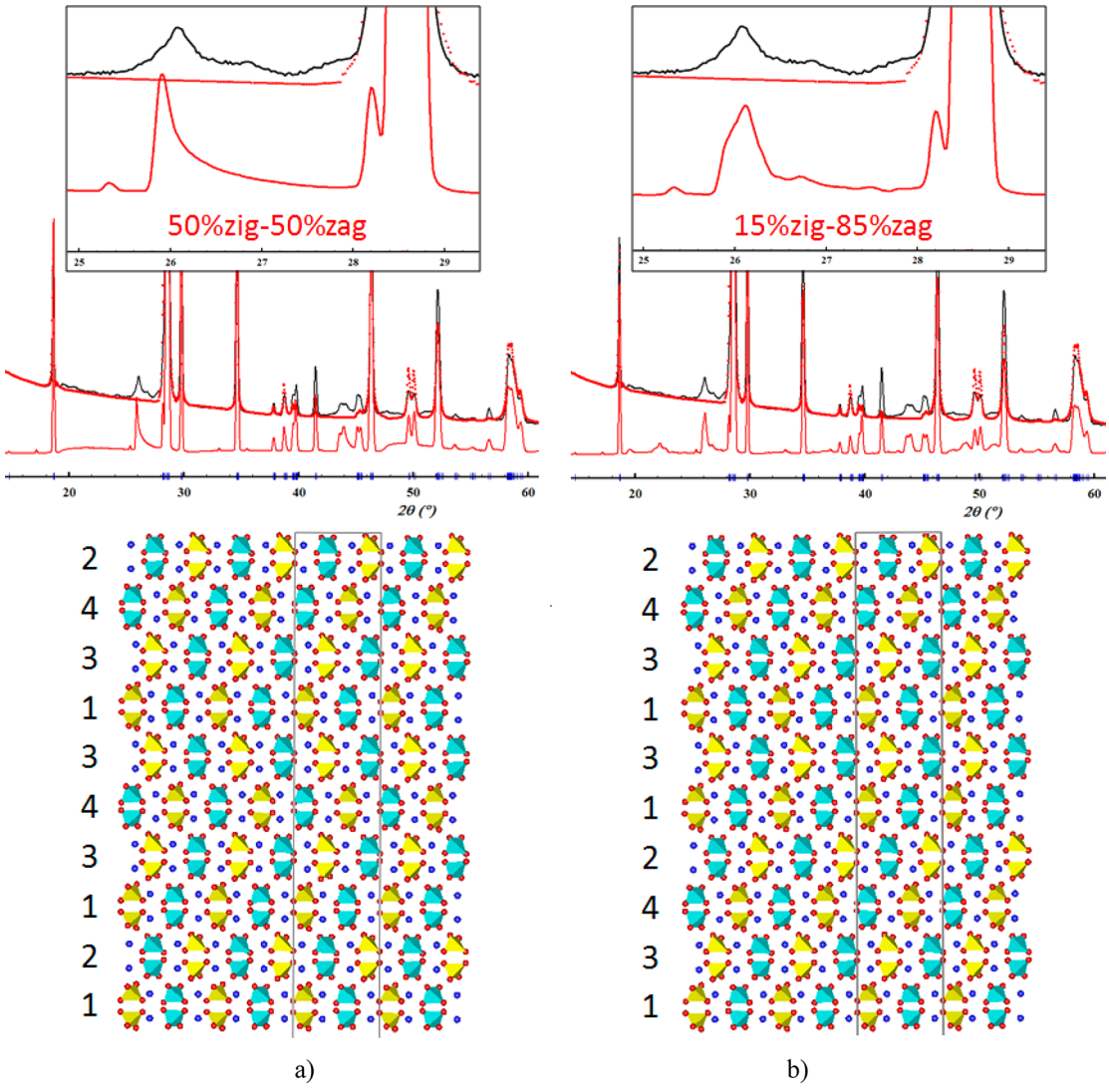

Figure 10. Two types of more (a) or less (b) random stacking disorder in model 1 of layers along the *b* axis (see Figure 7b) and their influence on the diffraction pattern and main extra diffraction peak (upper parts). In diffraction patterns: black line = observed; red dots = fit in a simple fergusonite cell with full Si/Mo disorder; red line = fit with given zigzag models.

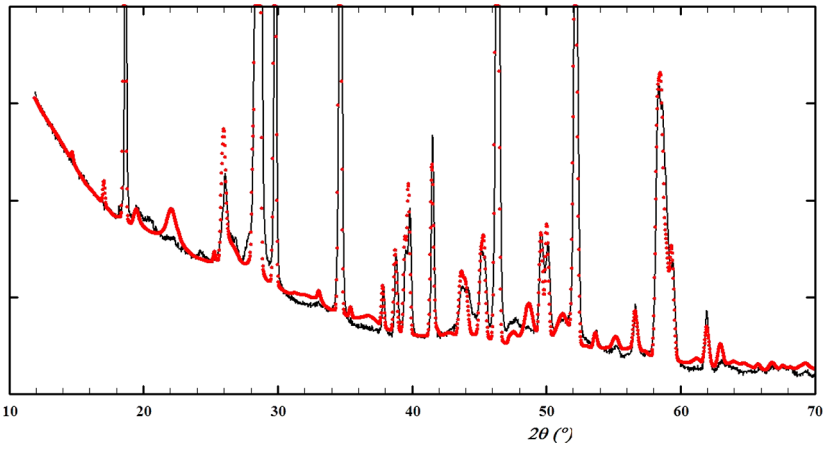

Figure 11. The X-ray powder diffraction patterns of DF-La_2SiMoO_8 (black line) and as simulated by FAULTS after refinement of the stacking model leading to a 15% zig–85% zag configuration (red dots). See text for comments.

consistent with a long-range order between the Si^{4+} and Mo^{6+} ions within each layer, that is to say two-dimensional in nature. Moreover our ultimate result suggesting a 15% zig–85% zag arrangement for DF-La_2SiMoO_8 is consistent with an intermediate situation between stacking disorder and stacking order, namely, in between 2D and 3D ordering for Si^{4+} and

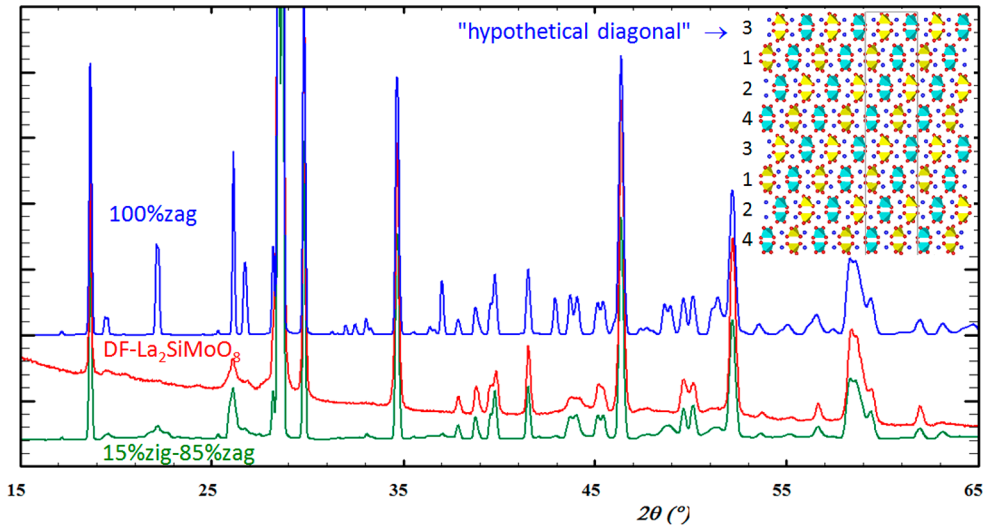

Figure 12. X-ray powder diffraction patterns of DF-La_2SiMoO_8 (red) and as simulated by FAULT for a 15% zig−85% zag model (green) and a fully ordered 100% zag model (blue), the "hypothetical diagonal" crystal structure of which is shown in the inset.

Mo^{6+} ions. This is obviously a high enough level of order to be detected by fluorescence spectroscopy.

As commented upon in the text about Figure 11, the proposed 15% zig−85% zag model duplicates correctly most of the features of the X-ray diffraction pattern, but not all of them perfectly. Accounting for, probably, additional defects such as layer stacking misorientation or partial shifts should be considered. Nevertheless, we hope that the current work will help with understanding the correlation between the structural order/disorder and the physical properties in multiple scheelites, and besides scheelites, in other materials the structure of which might be affected by layer stacking faults.

■ ASSOCIATED CONTENT

Accession Codes

CCDC 2046177 contains the supplementary crystallographic data for this paper. These data can be obtained free of charge via www.ccdc.cam.ac.uk/data_request/cif, or by emailing data_request@ccdc.cam.ac.uk, or by contacting The Cambridge Crystallographic Data Centre, 12 Union Road, Cambridge CB2 1EZ, UK; fax: +44 1223 336033.

■ AUTHOR INFORMATION

Corresponding Author

Philippe Lacorre − *Institut des Molécules et Matériaux du Mans (IMMM), UMR 6283 CNRS, Le Mans Université, F-72085 Le Mans Cedex 9, France;* orcid.org/0000-0003-1148-6694; Email: philippe.lacorre@univ-lemans.fr

Authors

Antoine Pautonnier − *Institut des Molécules et Matériaux du Mans (IMMM), UMR 6283 CNRS, Le Mans Université, F-72085 Le Mans Cedex 9, France*

Sandrine Coste − *Institut des Molécules et Matériaux du Mans (IMMM), UMR 6283 CNRS, Le Mans Université, F-72085 Le Mans Cedex 9, France*

Maud Barré − *Institut des Molécules et Matériaux du Mans (IMMM), UMR 6283 CNRS, Le Mans Université, F-72085 Le Mans Cedex 9, France*

Emilie Béchade − *Institut de Recherche sur les Céramiques (IRCER), UMR 7315 CNRS, Université de Limoges, Centre Européen de la Céramique, F-87068 Limoges Cedex, France*

Emmanuelle Suard − *Institut Laue Langevin (ILL), F-38042 Grenoble Cedex 9, France*

Complete contact information is available at: https://pubs.acs.org/10.1021/acs.inorgchem.0c03491

Notes

The authors declare no competing financial interest.

■ ACKNOWLEDGMENTS

The authors thank Dr. Juan Rodriguez-Carvajal (ILL) for his advice concerning the proper use of the program FAULTS.

■ REFERENCES

(1) Campos, A. B.; Simoes, A. Z.; Longo, E.; Varela, J. A.; Longo, V. M.; de Figueiredo, A. T.; De Vicente, F. S.; Hernandes, A. C. Mechanisms behind blue, green, and red photoluminescence emissions in $CaWO_4$ and $CaMoO_4$ powders. *Appl. Phys. Lett.* **2007**, *91* (5), 051923.

(2) Marques, A. P. A.; Motta, F. V.; Leite, E. R.; Pizani, P. S.; Varela, J. A.; Longo, E.; de Melo, D. M. A. Evolution of photoluminescence as a function of the structural order or disorder in $CaMoO_4$ nanopowders. *J. Appl. Phys.* **2008**, *104* (4), 043505.

(3) Sleight, A. W. Crystal Chemistry and Catalytic Properties of Oxides with the Scheelite Structure. In *Advanced Materials in Catalysis*; Burton, J. J., Garten, R. L., Eds.; Academic Press: New York, 1977; pp 181−208.

(4) Jeitschko, W. Crystal structure of $La_2(MoO_4)_3$, a new ordered defect scheelite type. *Acta Crystallogr., Sect. B: Struct. Crystallogr. Cryst. Chem.* **1973**, *29* (OCT15), 2074−2081.

(5) Brize, V.; Georges, S.; Kodjikian, S.; Suard, E.; Goutenoire, F. $La_6Mo_8O_{33}$: a new ordered defect Scheelite superstructure. *J. Solid State Chem.* **2004**, *177* (7), 2617−2627.

(6) Arakcheeva, A.; Chapuis, G. Capabilities and limitations of a (3+d)-dimensional incommensurately modulated structure as a model for the derivation of an extended family of compounds: example of the scheelite-like structures. *Acta Crystallogr., Sect. B: Struct. Sci.* **2008**, *64*, 12−25.

(7) Arulnesan, S. W.; Kayser, P.; Kimpton, J. A.; Kennedy, B. J. Studies of the fergusonite to scheelite phase transition in $LnNbO_4$ orthoniobates. *J. Solid State Chem.* **2019**, *277*, 229−239.

(8) Klevtsov, P. V.; Klevtsova, R. F. Polymorphism of the double molybdates and tungstates of mono- and trivalent metals with composition $M^+R^{3+}(EO_4)_2$. *J. Struct. Chem.* **1977**, *18* (3), 339−355.

(9) Kolesov, B. A.; Kozeeva, L. P. Raman study of cation distribution in the scheelite-like double molybdates and tungstates. *J. Struct. Chem.* **1994**, *34* (4), 534−539.
(10) Jeitschko, W.; Sleight, A. W.; McClellan, W. R.; Weiher, J. F. Comprehensive Study of Disordered and Ordered Scheelite-related $Bi_3(FeO_4)(MoO_4)_2$. *Acta Crystallogr., Sect. B: Struct. Crystallogr. Cryst. Chem.* **1976**, *32* (APR15), 1163−1170.
(11) Blasse, G. Crystal structure and fluorescence of compounds $Ln_2Me^{4+}Me^{6+}O_8$. *J. Inorg. Nucl. Chem.* **1968**, *30* (8), 2091−2099.
(12) Fukuda, K.; Asaka, T.; Hamaguchi, R.; Suzuki, T.; Oka, H.; Berghout, A.; Bechade, E.; Masson, O.; Julien, I.; Champion, E.; Thomas, P. Oxide-Ion Conductivity of Highly c-Axis-Oriented Apatite-Type Lanthanum Silicate Polycrystal Formed by Reactive Diffusion between La_2SiO_5 and $La_2Si_2O_7$. *Chem. Mater.* **2011**, *23* (24), 5474−5483.
(13) Lacorre, P.; Goutenoire, F.; Bohnke, O.; Retoux, R.; Laligant, Y. Designing fast oxide-ion conductors based on $La_2Mo_2O_9$. *Nature* **2000**, *404* (6780), 856−858.
(14) Boultif, A.; Louer, D. Indexing of Powder Diffraction Patterns for Low-Symmetry Lattices by the Successive Dichotomy Method. *J. Appl. Crystallogr.* **1991**, *24*, 987−993.
(15) Laugier, J.; Filhol, A. *CELREF: Unit-cell refinement software from powder diffraction data*, 1978.
(16) Sheldrick, G. M. A short history of SHELX. *Acta Crystallogr., Sect. A: Found. Crystallogr.* **2008**, *64*, 112−122.
(17) Le Bail, A.; Duroy, H.; Fourquet, J. L. Ab-initio Structure Determination of $LiSbWO_6$ by X-Ray Powder Diffraction. *Mater. Res. Bull.* **1988**, *23* (3), 447−452.
(18) Rodriguez-Carvajal, J. Recent Advances in Magnetic Structure Determination by Neutron Powder Diffraction. *Phys. B* **1993**, *192* (1−2), 55−69.
(19) Rodriguez-Carvajal, J. Recent developments of the program FULLPROF. *Commission on Powder Diffraction (IUCr) Newsletter* **2001**, *26*, 12−19.
(20) Treacy, M. M. J.; Newsam, J. M.; Deem, M. W. A General Recursion Method for calculating Diffracted Intensities from Crystals containing Planar Faults. *P. R. Soc.-Math. Phys. Sci.* **1991**, *433* (1889), 499−520.
(21) Casas-Cabanas, M.; Reynaud, M.; Rikarte, J.; Horbach, P.; Rodriguez-Carvajal, J. FAULTS: a program for refinement of structures with extended defects. *J. Appl. Crystallogr.* **2016**, *49*, 2259−2269.
(22) Putz, H.; Brandenburg, K. *Diamond - Crystal and Molecular Structure Visualization*; Crystal Impact GbR: Bonn, Germany. http://www.crystalimpact.com/diamond.
(23) Chapon, L.; Rodriguez-Carvajal, J. *FullProf Studio*, version 2.0, 2008.
(24) Klevtsova, R. F.; Soloveva, L. P.; Vinokurov, V. A.; Klevtsov, P. V. Crystal structure and polymorphism of rubidium-bismuth molybdate $RbBi(MoO_4)_2$. *Kristallografiya* **1975**, *20* (2), 270−275.